A study of cumulant approximations to n-electron valence multireference perturbation theory

Dominika Zgid, Debashree Ghosh, Eric Neuscamman, and Garnet Kin-Lic Chan

Citation: J. Chem. Phys. **130**, 194107 (2009); doi: 10.1063/1.3132922
View online: http://dx.doi.org/10.1063/1.3132922
View Table of Contents: http://aip.scitation.org/toc/jcp/130/19
Published by the American Institute of Physics

A study of cumulant approximations to *n*-electron valence multireference perturbation theory

Dominika Zgid,[a] Debashree Ghosh, Eric Neuscamman, and Garnet Kin-Lic Chan
Department of Chemistry and Chemical Biology, Cornell University, Ithaca, New York 14853-1301, USA

(Received 9 January 2009; accepted 21 April 2009; published online 18 May 2009)

We investigate the possibility of reducing the complexity of multireference perturbation theory through cumulant based approximations to the high-order density matrices that appear in such theories. Our test cases show that while the cumulant approximated forms are degraded in accuracy relative to the parent theory and exhibit intruder state problems that must be carefully handled, they may provide a route to a simple estimation of dynamic correlation when the parent perturbation theory is infeasible. Nonetheless, further work is clearly needed on better approximations to the denominators in the perturbation theory. © *2009 American Institute of Physics*.
[DOI: 10.1063/1.3132922]

I. INTRODUCTION

Electron correlation is generally understood to be divided into two kinds: nondynamic correlation, involving electron configurations distributed across "active" valence orbitals, and dynamic correlation, involving electron configurations with variable occupancy in "inactive" core and virtual orbitals. Dynamic correlation is generally a smaller, quantitative correction to the qualitative electronic structure that is established in the active valence space. For this reason, perturbation theory, even at the second-order level, is a practical tool to treat dynamical correlation. Perturbation theory on top of an arbitrary set of configurations in the valence space is known as multireference perturbation theory. The most popular forms today are the complete active space second-order perturbation (CASPT2) theory[1] and multireference Moller–Plesset perturbation (MRMP) theory[2] and more recently, second-order *n*-electron valence perturbation (NEVPT2) theory.[3,4] The difference between the CASPT2 and MRMP lies in the contraction of the basis states that span the first-order wave function. In CASPT2, the basis states are linear combinations of determinants [or configuration state functions (CSfs)] since single and double excitations are applied to the reference wave function, while in MRMP the states that span the first-order wave function are doubly excited determinants obtained from the determinants in the reference wave function. Thus, in MRMP the first-order interacting space is uncontracted. In strongly contracted NEVPT2 (SC-NEVPT2), the first-order wave function is spanned by vectors that are obtained from the contracted single and double excitation operators acting on the reference wave function. Consequently, the basis present in SC-NEVPT2 has a greater level of contraction than the CASPT2 or MRMP basis.

Despite the many predictive successes of multireference perturbation theory, such methods face a number of limitations. A severe one is the high computational cost as a function of the number of active orbitals, which prohibits their application to large molecules with many active orbitals. For example, current implementations of NEVPT2 are limited to 14 active orbitals, but much larger active spaces are accessible through methods such as the density matrix renormalization group (DMRG),[5–12] restricted active space self-consistent field (RASSCF),[13] or generalized valence bond (GVB) methods.[14] Improved algorithms (in particular, efficient choices of when to employ internal contraction[15]) ameliorate but do not remove the sharp increase in complexity of the multireference perturbation theory as the number of active orbitals and determinantal configurations increases.

In the current work, we explore the possibility of constructing approximate forms of multireference perturbation theory which are not at the outset limited to small active spaces. We take as our starting point the *n*-electron valence perturbation theory in its strongly contracted form (SC-NEVPT2), which is one of the simplest (and yet still remarkably successful) multireference perturbation theories available.[16] The basic idea of the work is quite simple. The complexity of multireference perturbation theories can be understood to arise from their dependence on contributions from high-order (three- and four-body) density matrices involving the active orbitals. We will explore the possibility of approximating these density matrices via the one- and two-body density matrices using cumulant-type expansions, removing any dependence on any more complex quantities. Naturally, this will introduce a degree of error, and the purpose of the work is to establish how tolerable such an error really is. To be successful, the error introduced by such cumulant-type approximations should not be larger than the intrinsic error of second-order multireference perturbation theory.

Cumulant approximations have been employed by many different workers in electronic structure.[17–21] In earlier work from our group, cumulant and operator decompositions have played a role in the formulation of the canonical transformation method, an exponential based description of dynamical correlation for multireference problems.[22–24] Unlike the

[a]Electronic mail: dominika.zgid@gmail.com.

stated objective of reduced density matrix methods, we are not trying here to use the cumulants as the primary variational descriptors of the electronic structure; instead, they are introduced as computational approximations to quantities that arise naturally in the multireference perturbation theory. Nonetheless, while our goals and presentation are different from some works in the reduced density matrix area, some differences can be viewed as simply matters of terminology and philosophy (e.g., is multireference perturbation theory to be described as a four-body density matrix energy functional or to be approximated as a two-body density matrix energy functional or as an internally contracted wave function based method where cumulants are used to approximate certain intermediates) and so there are many natural connections.

II. THEORY

A. Strongly contracted *n*-electron valence perturbation theory

We present a brief review of NEVPT2 theory. Our presentation closely follows that given in Ref. 3. Readers interested in more details should refer to the original articles[3,25,26] as well as the recent short review by Angeli *et al.*[4]

NEVPT2 is a second-order Rayleigh–Schrödinger perturbation theory, which differs from other kinds of multireference perturbation theory such as CASPT2 in its choice of zeroth-order Hamiltonian and the representation of the first-order wave function. Consider the zeroth-order wave function $\Psi^{[0]}$ (with zeroth-order energy $E^{[0]}$) which is the solution of some complete active space configuration interaction (CASCI) problem [typically obtained through a complete active space self-consistent field (CASSCF) problem]. We first establish some notation. We shall refer to core orbitals (doubly occupied in all CASCI configurations), active orbitals (variable occupancy in all CASCI configurations), and virtual orbitals (unoccupied in all CASCI configurations). Core orbitals will be associated with labels $i,j,k\ldots$, active orbitals with labels $a,b,c\ldots$, and virtual orbitals with labels $r,s,t\ldots$. We define a *model* Hamiltonian known as the Dyall Hamiltonian,[27] which consists of Fock-type operators in the core and virtual spaces and the Hamiltonian H_{act} in the active space, i.e.,

$$H^D = f_{\mathrm{core}} + H_{\mathrm{act}} + f_{\mathrm{ext}}, \tag{1}$$

$$f_{\mathrm{core}} = \sum_i \epsilon_i a_i^\dagger a_i + C, \tag{2}$$

$$H_{\mathrm{act}} = \sum_{ab\in \mathrm{act}} h_{ab}^{\mathrm{eff}} a_a^\dagger a_b + \sum_{abcd\in \mathrm{act}} v_{abcd} a_a^\dagger a_b^\dagger a_c a_d, \tag{3}$$

$$f_{\mathrm{ext}} = \sum_r \epsilon_r a_r^\dagger a_r, \tag{4}$$

$$H^D \Psi^{[0]} = E^{[0]} \Psi^{[0]}. \tag{5}$$

Note that the one-body part of H_{act} includes the Coulomb field from the core electrons, i.e., $h_{ab}^{\mathrm{eff}} = h_{ab} + \Sigma_{i\in \mathrm{core}}(ii|ab) - (ia|ib)$, and C is a constant chosen so that the expectation value of the Dyall Hamiltonian with $\Psi^{[0]}$ is the CASCI energy. The core and virtual orbitals are taken to be canonical orbitals of Fock operators defined using CASCI one-particle density matrices. The two-body integrals in the molecular orbital basis are denoted by v_{abcd}.

In the so-called SC-NEVPT2 which is of interest here, the first-order wave function $\Psi^{[1]}$ is expanded in terms of a *highly restricted* set of "perturber" functions. These are classified into eight spaces, (0), (+1), (−1), (+2), (−2), (+1)′, (−1)′, and (0)′, which differ by the pattern of excitations involving core and virtual orbitals and the number of particles or holes introduced into the active space. [The number (+1), for example, denotes one particle introduced into the active space. Note also that we are using parentheses to label these eight spaces, whereas brackets are used to denote orders of perturbation theory.]

The perturber functions in each of the eight spaces are contracted sets of determinants, where the contraction coefficients are defined from the perturbation V. We first divide V into eight components which connect the reference wave function and the eight different spaces,

$$V = \sum_{i<j,r<s} V_{ijrs}^{(0)} + \sum_{i<j,r} V_{ijr}^{(+1)} + \sum_{r<s,i} V_{rsi}^{(-1)} + \sum_{i<j} V_{ij}^{(+2)} + \sum_{r<s} V_{rs}^{(-2)} + \sum_i V_i^{(+1)'} + \sum_r V_r^{(-1)'} + \sum_{ir} V_{ir}^{(0)'}, \tag{6}$$

where the eight component perturbations are defined through (using the compact second-quantized notation, e.g., $a_{ij}^{rs} = a_r^\dagger a_s^\dagger a_i a_j$)

$$V_{ijrs}^{(0)} = \langle rs||ji\rangle a_{ij}^{rs}, \tag{7}$$

$$V_{ijr}^{(+1)} = \sum_a \langle ra||ji\rangle a_{ij}^{ra}, \tag{8}$$

$$V_{rsi}^{(-1)} = \sum_a \langle rs||ia\rangle a_{ai}^{rs}, \tag{9}$$

$$V_{ij}^{(+2)} = \sum_{a<b} \langle ab||ji\rangle a_{ij}^{ab}, \tag{10}$$

$$V_{rs}^{(-2)} = \sum_{a<b} \langle rs||ba\rangle a_{ab}^{rs}, \tag{11}$$

$$V_i^{(+1)'} = \sum_{a<b,c} \langle ab||ic\rangle a_{ci}^{ab} + \sum_{aj} \langle aj||ij\rangle a_{ji}^{aj} + \sum_a \langle a|h|i\rangle a_i^a, \tag{12}$$

$$V_r^{(-1)'} = \sum_{a,b<c} \langle ra||cb\rangle a_{bc}^{ra} + \sum_{aj} \langle rj||aj\rangle a_{ja}^{rj} + \sum_a \langle r|h|a\rangle a_a^r, \tag{13}$$

$$V_{ir}^{(0)'} = \sum_{ab} \langle ra||ib\rangle a_{bi}^{ra} + \sum_j \langle rj||ij\rangle a_{ji}^{rj} + \langle r|h|i\rangle a_i^r. \tag{14}$$

Note that orbital labels of the component perturbations refer to only inactive (core or virtual) orbitals; all active indices are summed over.

The perturber functions are then generated by applying each of the component perturbations to the zeroth-order wave function and normalizing. Thus, the eight classes of perturber functions are

$$\Phi_{ijrs}^{(0)} = \frac{1}{\sqrt{N_{ijrs}^{(0)}}} V_{ijrs}^{(0)} \Psi^{[0]}, \tag{15}$$

$$\Phi_{ijr}^{(+1)} = \frac{1}{\sqrt{N_{ijr}^{(+1)}}} V_{ijr}^{(+1)} \Psi^{[0]}, \tag{16}$$

and so on, where we have introduced the square norm, e.g., $N_{ijr}^{(+1)} = \langle \Psi^{[0]} | V_{ijr}^{(+1)\dagger} V_{ijr}^{(+1)} | \Psi^{[0]} \rangle$. Note that every perturber function is orthogonal to every other perturber function. Consequently, in contrast to internally contracted CASPT2 or partially contracted NEVPT2, there is no need for diagonalization of the overlap matrix between perturber functions. This feature of the strongly contracted theory is advantageous if we want to perform calculations with a large active space (e.g., with DMRG or another method), where the overlap diagonalization may prove to be a bottleneck.

Now that we have defined the perturber functions, we can specify the zeroth-order Hamiltonian used in SC-NEVPT2. This is of the form

$$H^{[0]} = P_{\text{act}} H^D P_{\text{act}} + \sum_{l,k} |\Phi_l^{(k)}\rangle E_l^{(k)} \langle \Phi_l^{(k)}|, \tag{17}$$

where $E_l^{(k)} = \langle \Phi_l^{(k)} | H^D | \Phi_l^{(k)} \rangle$, P_{act} projects onto the active space, and the functions $|\Phi_l^{(k)}\rangle$ are the perturber functions.

In terms of the perturber functions, the first-order wave function is expanded as

$$\Psi^{[1]} = \sum_{i<j,r<s} c_{ijrs}^{(0)} \Phi_{ijrs}^{(0)} + \sum_{i<j,r} c_{ijr} \Phi_{ijr}^{(+1)} + \cdots. \tag{18}$$

The coefficients and energy contribution can be obtained using the standard Rayleigh–Schrödinger expressions, evaluated in sum-over-states form. Taking the (+1) subspace as an example [and dropping the (+1) labels below for convenience], we have

$$c_{ijr} = -\frac{\langle \Phi_{ijr} | V | \Psi \rangle}{E_{ijr} - E^{[0]}} = -\frac{\langle \Phi_{ijr}^{(+1)} | V_{ijr}^{(+1)} | \Psi \rangle}{E_{ijr} - E^{[0]}} = -\frac{\sqrt{N_{ijr}}}{E_{ijr} - E^{[0]}}, \tag{19}$$

$$E^{[2]} = -\sum_{i<j,r} \frac{N_{ijr}}{E_{ijr} - E^{[0]}}, \tag{20}$$

where E_{ijr} is the zeroth-order energy of the perturber function, i.e., $\langle \Phi_{ijr}^{(+1)} | H^{[0]} | \Phi_{ijr}^{(+1)} \rangle$.

B. Cumulant approximated strongly contracted NEVPT2

Evaluating matrix elements in NEVPT2 for the coefficients and for the energy contributions is not a simple matter computationally. This can be understood because matrix elements involving perturber functions that allow active orbital relaxation [i.e., semi-internal-type excitations in $(+1)'$ and $(-1)'$ spaces of the form $a_{ab}^{rc}|\Psi\rangle$] involve long strings of active orbital operators. We can examine the complexity of NEVPT2 by reducing all matrix element expressions to traces of reduced density matrices with appropriate integrals. Depending on the subspace in NEVPT2, different density matrices are involved (see Table I) but in the worst case [for the $(-1)'$ and $(+1)'$ subspaces], just as in other multireference perturbation theories such as CASPT2, four-particle reduced density matrices formally appear. This greatly increases the complexity of these multireference perturbation theories relative to the single-reference counterpart, Moller–Plesset theory. For example, the computational scaling of the NEVPT2 implementation described in Ref. 25 is $O(n_{\text{act}}^9)$ to construct the intermediate expressions in subspaces $(+1)'$ and $(-1)'$. This presents a fundamental limitation if we wish to use the NEVPT2 method in conjunction with a reference function obtained in a large active space. As noted in the early articles on NEVPT2,[3] the theory is general and can in principle be combined with non-CASCI references (such as a GVB reference or a DMRG reference) which are not limited to the small active spaces of CASCI.

TABLE I. Highest rank reduced density matrices appearing in the energy contributions for the eight subspaces of NEVPT2. The energy expression involves a numerator and denominator (see, e.g., Ref. 20); the highest rank reduced density matrices contributing to the numerator and denominator separately are shown in columns 3 and 4. Active space density matrices do not contribute to the energy of the (0) space.

Subspace	All	Numerator	Denominator
(0)	n.a.	n.a.	n.a.
(+1)	2	1	2
(−1)	2	1	2
(+2)	3	2	3
(−2)	3	2	3
$(+1)'$	4	3	4
$(-1)'$	4	3	4
$(0)'$	3	2	3

One way to reduce the complexity of NEVPT2 theory (and multireference perturbation theories in general) is to remove the explicit or implicit dependence of the energy expressions on high particle density matrices. (By implicit dependence, we refer to such algorithms, often used in CASPT2 implementations, where the higher particle density matrices are not explicitly constructed and instead where their contributions are computed directly on the fly using the determinantal expansion of the CASCI wave function.) Ideally we would hope that no quantities more complex than the one- and two-particle active space density matrices should appear. This is achieved in the following cumulant approximated strongly contracted NEVPT2 (cu-SC-NEVPT2) and cumulant with diagonals approximated strongly contracted NEVPT2 (cud-SC-NEVPT2) methods.

1. cu-SC-NEVPT2

In the cu-SC-NEVPT2 approximation, we use cumulant approximations of the three- and four-particle density matrices in terms of the one- and two-particle density matrices. For the density matrices, we use the notation $\gamma_{def}^{abc} = \langle a_{def}^{abc} \rangle$. These approximations are then given as

$$\gamma^{abc}_{def} \Rightarrow \sum (-1)^x \gamma^a_d \gamma^{bc}_{ef} \ (9 \ \text{terms}) - 2 \sum (-1)^x \gamma^a_d \gamma^b_e \gamma^c_f \ (6 \ \text{terms})$$

$$= \gamma^a_d \gamma^{bc}_{ef} - \gamma^a_e \gamma^{bc}_{df} + \gamma^a_f \gamma^{bc}_{de} - \gamma^b_d \gamma^{ac}_{ef} + \gamma^b_e \gamma^{ac}_{df} - \gamma^b_f \gamma^{ac}_{de} + \gamma^c_d \gamma^{ac}_{ef} - \gamma^c_e \gamma^{ac}_{df} + \gamma^c_f \gamma^{ac}_{de} - 2(\gamma^a_d \gamma^b_e \gamma^c_f - \gamma^a_d \gamma^c_e \gamma^b_f + \gamma^b_d \gamma^c_e \gamma^a_f - \gamma^b_d \gamma^a_e \gamma^c_f + \gamma^c_d \gamma^a_e \gamma^b_f - \gamma^c_d \gamma^b_e \gamma^a_f), \tag{21}$$

$$\gamma^{abcd}_{efgh} \Rightarrow \sum (-1)^x \gamma^{ab}_{ef} \gamma^{cd}_{gh} \ (18 \ \text{terms}) - 2 \sum (-1)^x \gamma^a_e \gamma^b_f \gamma^c_g \gamma^d_h \ (24 \ \text{terms}). \tag{22}$$

Note that in the case of the four-particle density matrix we have not written out all terms explicitly, but these can be obtained by attaching appropriate signs to the additional contributions arising from permutation of indices: this is denoted by the parity factor $(-1)^x$ which takes the appropriate +1 and −1 signs according to the permutation. To obtain the cu-SC-NEVPT2 energy and coefficients, we simply substitute the approximate three- and four-particle density matrices as defined above into the matrix element expressions in NEVPT2 (e.g., as defined in the Appendix of Ref. 25). Note that the contributions of subspaces (0), (+1), and (−1) are not affected by the cumulant approximation.

2. cud-SC-NEVPT2

To improve on the cu-SC-NEVPT2, we have investigated a better approximation to the three- and four-particle density matrices. In a typical basis, the largest elements of the three-particle and four-particle density matrices occur along the diagonals and thus it would appear most important to include information about these elements first. This can be done by incorporating the exact three- and four-particle diagonal elements of the density matrices. This does not increase the complexity of the theory over that of cu-SC-NEVPT2 since the number of four-particle diagonal elements (from which the three-particle diagonals are readily obtained) is n^4_{act}, which is the same number of elements as in the two-particle density matrix. We can also incorporate some additional information of the same complexity concerning the off-diagonal elements of the three- and four-particle density matrices, as long as we consider subsets of elements which are labeled by four indices or fewer. Thus, in the cud-SC-NEVPT2 theory, we construct the three-particle density matrix via the cumulant approximation (22) but then replace selected diagonal and off-diagonal terms with their exact values, in particular, elements $\gamma^{abc}_{abc}, \gamma^{abc}_{bac}, \gamma^{abc}_{cab}, \ldots$. In the case of the four-particle density matrix, since we now have explicit information from the three-particle density matrix beyond the cumulant approximation, to be consistent we construct the four-particle density matrix from its cumulant expansion in terms of one-, two-, and three-particle density matrices where the three-particle density matrix has been corrected as above. This expansion is given by

$$\gamma^{abcd}_{efgh} = \sum (-1)^x \gamma^a_e \gamma^{bcd}_{fgh} \ (16 \ \text{terms}) + \sum (-1)^x \gamma^{ab}_{ef} \gamma^{cd}_{gh} \ (18 \ \text{terms}) - 2 \sum (-1)^x \gamma^a_e \gamma^b_f \gamma^{cd}_{gh} \ (72 \ \text{terms}) + 6 \sum (-1)^x \gamma^a_e \gamma^b_f \gamma^c_g \gamma^d_h \ (24 \ \text{terms}). \tag{23}$$

From this cumulant approximated four-particle density matrix, we then replace the following four-indexed diagonal and off-diagonal elements with their exact values, $\gamma^{abcd}_{abcd}, \gamma^{abcd}_{bacd}, \gamma^{abcd}_{cabd}, \ldots$.

In our implementation the four-particle density matrix is not kept in memory due to earlier precontraction with integrals of the one-, two-, and three-particle density matrices used in the cumulant expansion, which lowers the overall computational scaling.

Note that there is a difference between our use of cumulants in NEVPT2 and their use in other methods in quantum chemistry such as the contracted Schrödinger equation (CSE) methods.[28–30] The CSE methods employ cumulant approximation in order to directly optimize one- and two-body reduced density matrices in both the active and external spaces without reference to an explicit wave function. These cumulant approximations can be problematic due to the dependence of the *n*-representability error on the basis set size, as explored by Harris[31] and Herbert.[32] Although in NEVPT2 the higher-order density matrices are approximated by cumulants, these higher-order density matrices are restricted only to the active space and are constructed to approximate the (physically correct) reference wave function active space density matrices. Consequently, in the cumulant approximated NEVPT2, one can expect that the quality of the cumulant approximation will not depend on the size of the basis set since the reference wave function density matrices for the active space change very little with respect to the basis size.

C. False intruders from cumulant approximations

Intruder states are perturber states (i.e., excited from the reference) which are near degenerate with the reference wave function with respect to the zeroth-order Hamiltonian (but are not so with the true Hamiltonian). They give rise to a zeroth-order problem which appears near degenerate when no such near degeneracy exists in the real system and are a common problem in multireference perturbation theories such as CASPT2. NEVPT2 theory was developed in part to

address the problem of intruder states. The use of the two-electron Hamiltonian in the active space (via the model Dyall Hamiltonian) ensures a better estimate of the relative energies of the perturber states and reference state, reducing the risk of possible intruders.

However, in the cumulant based approximations that we have introduced, problems with small denominators can reappear. While such problems appear to be similar to the ones caused by intruder states, it is important to note that their origin is very different. The "true intruder" states present in CASPT2 arise because of weakly interacting states that are quasidegenerated at the zeroth order with the reference state. On contrary, in cumulant approximated NEVPT2 the convergence problems appear because the energy denominators are no longer evaluated exactly, and the errors of the cumulant approximation may lead to falsely small denominators. We refer to these divergences as "false intruders" because they are a pure artifact of the error made in the cumulant approximation. Consider, for example, the expression for the second-order energy in the $(-1)'$ subspace. Rewriting Eq. (20) using the fact that $H_{\mathrm{act}}\Psi^{[0]}=E^{[0]}\Psi^{[0]}$, we have

$$E^{[2]} = -\sum_r \frac{N_r}{E_r - E^{[0]}} = -\sum_r \frac{N_r}{\epsilon_r - \frac{1}{N_r}\langle\Psi^{[0]}|V_r^{(-1)'\dagger}[H_D, V_r^{(-1)'}]|\Psi^{[0]}\rangle}. \quad (24)$$

Both the numerator and the denominator are approximated, the numerator requiring a three-particle density matrix and the denominator (by virtue of the $\langle\Psi^{[0]}|V_r^{(-1)'\dagger}[H_D, V_r^{(-1)'}]|\Psi^{[0]}\rangle$ term) requiring a four-particle density matrix. We can imagine two kinds of errors introduced by the cumulant approximation to the denominator. In the first case, the denominators may all simply be poor, e.g., somewhat shifted, but no divergences occur. In the second case, the cumulant approximation to $(1/N_r)\times\langle\Psi^{[0]}|V_r^{(-1)'\dagger}[H_D, V_r^{(-1)'}]|\Psi^{[0]}\rangle \approx \epsilon_r$ and a false intruder appears, with a corresponding divergent contribution to the energy.

To ameliorate the effects of possible false intruders, we have incorporated level shifts into our cu-SC-NEVPT2 and cud-SC-NEVPT2 methods. We use imaginary level shifts as investigated by Forsberg and Malmqvist.[33] When using the level shift, we have also evaluated the cumulant approximated NEVPT2 energies using the level-shift corrected energy expression of Ref. 33, which is designed to minimize the effect of the level shift when there are no intruder states. The correction corresponds to evaluating the second-order energy from the Hylleraas functional with the first-order wave function coefficients determined with the level shift. Note that when using level shifts with cu-SC-NEVPT2 we need not apply the level shift to every subspace; only the subspace in which the false intruder is observed. In the tables and figures, we list the value of the level shift in parentheses, e.g., cu-SC-NEVPT2(0.2) means the value of the applied imaginary level shift was $0.2i$ a.u.

III. TEST CASES

We have incorporated the cu-SC-NEVPT2 and cud-SC-NEVPT2 approximations into the existing NEVPT2 implementation in the development version of DALTON.[34] To assess the accuracy of these approximations, we have studied a number of benchmark quantum chemistry problems: the singlet-triplet gap of CH_2 and SiH_2, the nitrogen and chromium dimer potential energy curves, and the excitation energies in short polyenes. Unless otherwise specified, benchmark results for ordinary SC-NEVPT2 were obtained with DALTON, while benchmark results for CASSCF, full configuration interaction (FCI), and CASPT2 were obtained with MOLPRO.[35] (In the MOLPRO CASPT2 calculation the "rs2" variant was used in all cases except for the polyenes, where the "rs2c" variant" was used.)

A. Test case I: Singlet-triplet gaps in CH_2 and SiH_2

As a first test of the accuracy of the cu-SC-NEVPT2 methods, we calculated the ground-state singlet-triplet splittings in CH_2 and SiH_2. These are small quantities and thus very sensitive to any errors made in the differential correlation between the singlet and triplet states. The same systems have been used in earlier studies to benchmark the accuracy of multireference perturbation theory.[16]

For CH_2, the geometry was taken from Ref. 36 and the basis set (double zeta with polarization quality) was also taken from Ref. 36. (Note that different polarization functions are used for the singlet and triplet states for CH_2.) The CASSCF consisted of $2a_1$, $3a_1$, $4a_1$, $1b_1$, $2b_1$, and $1b_2$ orbitals. The $1a_1$ orbital was a core orbital (always doubly occupied) in the CASSCF calculation and was treated as frozen (i.e., an uncorrelated orbital) in all NEVPT2, CASPT2, and FCI calculations. The energies of the $^1A_1$ and ^3B_u states were obtained at the state-specific CASSCF level, and these states were subsequently used in the NEVPT2 and CASPT2 calculations.

For SiH_2, the geometry was taken from Ref. 37 and the basis set (which was of double zeta with polarization quality) was also taken from Ref. 37. The CASSCF consisted of $4a_1$, $5a_1$, $6a_1$, $2b_1$, $3b_1$, $2b_2$ orbitals, with all lower orbitals held as core orbitals in the CASSCF calculation and frozen in subsequent NEVPT2, CASPT2, and FCI calculations. The energies of the $^1A_1$ and ^3B_u states were obtained at the state-specific CASSCF level, and these states were subsequently used in the NEVPT2 and CASPT2 calculations.

1. Discussion

As can be seen from Tables II and III, the pure cumulant based cu-SC-NEVPT2 result is poorly balanced between the singlet and triplet states, while the cumulant with diagonals cud-SC-NEVPT2 approximation performs significantly better. In fact, the cu-SC-NEVPT2 gaps are worse than the CASSCF gaps! The cud-SC-NEVPT2 gaps are of similar quality (relative to the FCI result) to the standard SC-NEVPT2 or CASPT2 singlet-triplet gaps.

To better understand the origin of the errors in the cumulant approximated methods, we can analyze the contributions to the errors from each subspace of the NEVPT2 cal-

TABLE II. Ground-state singlet-triplet gap in CH_2 (see text for basis and geometry).

Method	Singlet energy (E_h)	Triplet energy (E_h)	Gap (kcal/mol)
FCI	−39.027 183	−39.046 229	11.95
CASSCF	−38.945 529	−38.965 954	12.82
CASPT2	−39.012 184	−39.037 061	15.61
SC-NEVPT2	−39.006 707	−39.028 498	13.67
cu-SC-NEVPT2(0.1)	−39.003 499	−39.042 508	24.48
cud-SC-NEVPT2(0.1)	−39.006 470	−39.029 253	14.30

TABLE III. Ground-state singlet-triplet gap in SiH_2 (see text for basis and geometry).

Method	Singlet energy (E_h)	Triplet energy (E_h)	Gap (kcal/mol)
FCI	−290.110 206	−290.082 219	17.50
CASSCF	−290.042 910	−290.016 811	16.38
CASPT2	−290.095 403	−290.071 351	15.09
SC-NEVPT2	−290.088 824	−290.062 222	16.69
cu-SC-NEVPT2(0.1)	−290.083 694	−290.072 706	6.90
cud-SC-NEVPT2(0.1)	−290.089 888	−290.064 103	16.18

culations, which we do now for the CH_2 singlet and triplet states. Since all the core orbitals are frozen (uncorrelated) in the CH_2 calculation, all correlation energies in subspaces that involve excitations from core orbitals vanish. This means that only subspaces (-2) and $(-1)'$ contribute to the correlation energy. We compare the first-order wave function norm and energy contributions of these subspaces for the singlet and triplet states and the various SC-NEVPT2 approximations in Table IV.

We see that in both cu-SC-NEVPT2 and cud-SC-NEVPT2, the first-order wave function norm and second-order energy contribution of the (-2) space are well approximated; errors in the correlation energy for this space are less than 0.5 mH. From Table I we recall that the (-2) subspace requires a three-particle cumulant approximation in the denominators appearing in the NEVPT2 coefficient and energy expressions. The largest errors arise in the $(-1)'$ space. In particular, the cu-SC-NEVPT2 correlation energy in this space for the triplet state is overestimated by −14 mH, giving rise to the spuriously large singlet-triplet gap. Consistent with this is the error in the wave function norm in this subspace, which is more than twice the correct norm. From Table I we recall that the $(-1)'$ subspace requires *both* three- and four-particle cumulant approximations, and is thus expected to be associated with larger errors.

We can further break up the error contribution by the error in the numerator and denominator of the sum-over-states expression for the energy [Eq. (24)]. Although the numerators that require at most the three-particle density matrix are approximated well using the cumulant approximation, the main source of error lies in the values of the denominators that are usually too small. In Fig. 1 we plot (as a function of virtual index) the denominators for the $(-1)'$ subspace in the SC-NEVPT2, cu-SC-NEVPT2, and cud-SC-NEVPT2 theories. While the cud-SC-NEVPT2 denominators appear to be close to the SC-NEVPT2 ones, the denominators obtained without introduction of the diagonal elements (i.e., for cu-SC-NEVPT2) seem to be too small for many of the virtual indices. It should be noted that one of the perturbers has a negative denominator. Such a behavior is an example of problems in the definition of the zero-order energies while using cumulants. However, although we see that errors in the denominators of the cu-SC-NEVPT2 expressions no doubt contribute to the overly large wave function norm and overestimated correlation energies in this subspace, we do not really have a case of a vanishing denominator and diverging energy (see Fig. 2) contribution due to a false intruder state. For this reason, the effect of a level-shift correction is quite small. Indeed, the cu-SC-NEVPT2 singlet-triplet gap calculated with imaginary level shifts of 0.1, 0.2, and 0.4 a.u. in the $(-1)'$ subspace, calculated with the corrected level-shift energies as in Ref. 33, remains to be 24.48 kcal/mol. One can see that a better estimation of the denominator is needed than that given by the pure cumulant approximation. It appears that for these systems, the primary errors in the cumulant approximation can be corrected by incorporating the additional "diagonal" elements, as used in the cud-SC-NEVPT2 method, and that this method gives a qualitatively balanced description of the dynamic correlation, but the results may be less satisfactory in other cases.

B. Test case II: Nitrogen and chromium potential energy curves

As a more stringent evaluation of the cu-SC-NEVPT2 and cud-SC-NEVPT2 approximations, we carried out calculations on the nitrogen and chromium binding curves. The correct description of multiple bond stretching is among the

TABLE IV. Subspace contributions to the correlation energy and wave function norm for various SC-NEVPT2 methods in the CH_2 molecule.

		SC-NEVPT2		cu-SC-NEVPT2		cud-SC-NEVPT2	
State	Subspace	Wave function norm	Energy (mE_h)	Wave function norm	Energy (mE_h)	Wave function norm	Energy (mE_h)
$^1A_1$	(-2)	7.5×10^{-3}	−31.8	8.4×10^{-3}	−31.3	7.4×10^{-3}	−31.7
	$(-1)'$	11.9×10^{-3}	−29.4	16.2×10^{-3}	−26.7	11.9×10^{-3}	−29.2
$^3B_1$	(-2)	6.9×10^{-3}	−30.9	6.9×10^{-3}	−30.9	6.9×10^{-3}	−30.9
	$(-1)'$	12.1×10^{-3}	−31.6	40.0×10^{-3}	−45.6	12.9×10^{-3}	−32.4

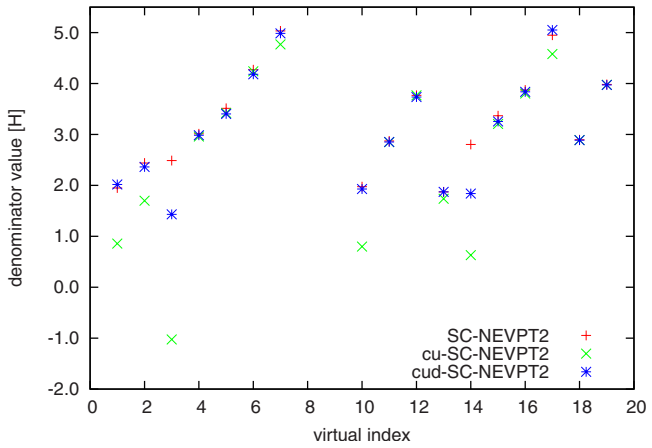

FIG. 1. (Color online) Energy denominators for respective virtual indices in the $(-1)'$ subspace for the $^3B_1$ state of CH_2 using SC-NEVPT2, cu-SC-NEVPT2, cud-SC-NEVPT2.

hardest problems in benchmark quantum chemistry. Furthermore, it is well known from CASPT2 studies that intruder state problems can arise at many geometries along such potential energy curves.[38]

For N_2 we studied the lowest singlet $^1\Sigma_g$ and lowest triplet $^3\Sigma_u$ states. We used Dunning, Jr.'s correlation consistent quadruple-zeta basis (cc-pVQZ) (Refs. 39 and 40) and the CASSCF consisted of all $2s$ and $2p$ orbitals ($10e$, eight orbitals) active space. The $1s$-derived orbitals were kept doubly occupied in the CASSCF reference and correlated in the subsequent CASPT2 and NEVPT2 calculations as core orbitals. For Cr_2 we studied the lowest singlet state using the Wachters+f atomic natural orbital basis[40–42] and a CASSCF active space containing all $3d$ and $4s$ orbitals—($12e$, 12 orbitals) active space. All other occupied orbitals were correlated as core orbitals.

1. Discussion

Shown in Fig. 3 is the $^1\Sigma_g$ binding curve of N_2 using both cu-SC-NEVPT2 and SC-NEVPT2 theories. What is immediately apparent is that the cu-SC-NEVPT2 curve has several divergences arising from false intruder states which do

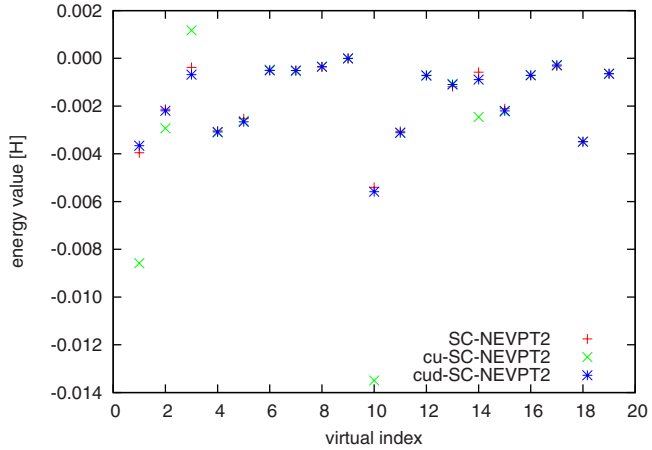

FIG. 2. (Color online) Energy contributions for respective virtual indices in the $(-1)'$ subspace for the $^3B_1$ state of CH_2 using SC-NEVPT2, cu-SC-NEVPT2, and cud-SC-NEVPT2.

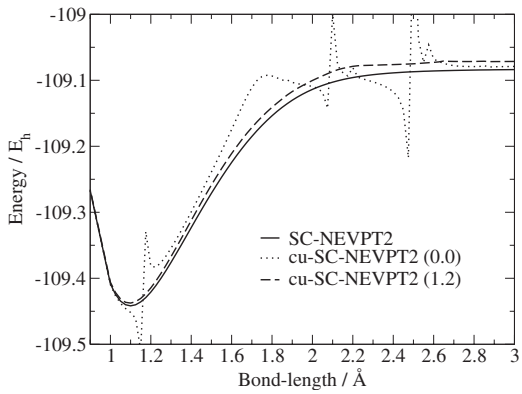

FIG. 3. $^1\Sigma_g$ binding curve of N_2 using cu-SC-NEVPT2 and NEVPT2 theories. The cu-SC-NEVPT2 calculations are carried out using a variety of imaginary level shifts in the $(-1)'$ subspace (value indicated in brackets).

not appear in the original SC-NEVPT2 theory. Such false intruder states occur even close to the equilibrium region but can be smoothed out by applying a sufficiently large imaginary level shift in the $(-1)'$ subspace. It is necessary to stress that these divergences appear because of the error made in the cumulant approximation of the three- and four-body density matrices present in the denominators of $(-1)'$ subspace. The physical meaning of such denominator contribution $(1/N_r)\langle\Psi^{[0]}|V_r^{(-1)'\dagger}[H_D, V_r^{(-1)'}]|\Psi^{[0]}\rangle$ is that of a generalized ionization energy, and, as observed in Fig. 1, the typical value of such energies in the parent SC-NEVPT2 theory is $O(1)$ a.u. Thus it is natural to require a level shift of this magnitude to correct divergences arising from the error in the cumulant approximation.

Consequently, the magnitude of the necessary level shift (1.2 a.u.) may seem rather large as compared to typical shifts employed in CASPT2 theory. Such a large level shift, however, does give rise to a significantly vertically shifted curve in the dissociation region.

In Fig. 4 is the corresponding $^1\Sigma_g$ binding curve of N_2 using cud-SC-NEVPT2 and SC-NEVPT2 theories. The cud-SC-NEVPT2 curve does not suffer from false intruders in the equilibrium region and instead closely follows the parent SC-NEVPT2 curve. However, at approximately 2.2 Å we observe divergences once again. These can be also smoothed

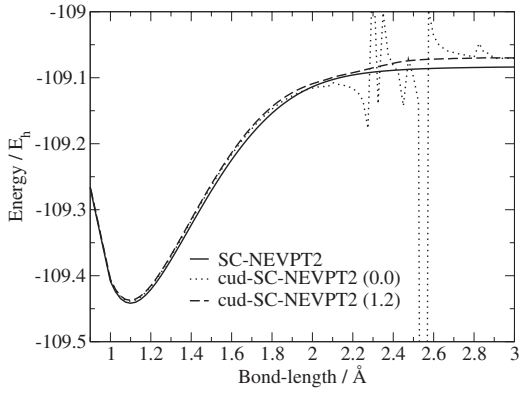

FIG. 4. $^1\Sigma_g$ binding curve of N_2 using cud-SC-NEVPT2 and NEVPT2 theories. The cu-SC-NEVPT2 calculations are carried out using a variety of imaginary level shifts in the $(-1)'$ subspace (value indicated in brackets).

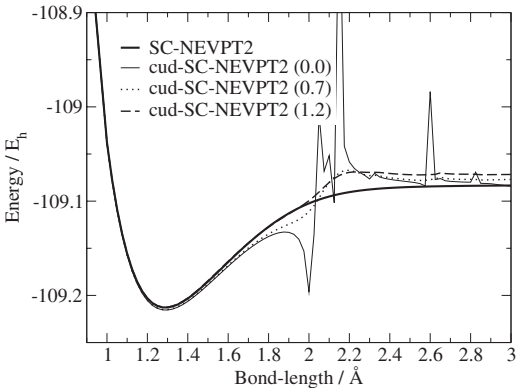

FIG. 5. $^3\Sigma_u$ binding curve of N_2 using cud-SC-NEVPT2 and NEVPT2 theories. The cud-SC-NEVPT2 calculations are carried out using a variety of imaginary level shifts in the $(-1)'$ subspace (value indicated in brackets).

out using an imaginary level shift, leading to a similarly vertically shifted curve in the dissociation region. In Fig. 5 we plot the $^3\Sigma_u$ binding curve of N_2 using cud-SC-NEVPT2 and SC-NEVPT2 theories. Note that unlike CASPT2 calculations in atomic natural orbital (ANO) basis sets,[38] SC-NEVPT2 does not exhibit any intruder problems for this state. As for the ground state, there are no false intruders in the cud-SC-NEVPT2 curve until one reaches the stretched region, near 2 Å. Although it is possible to remove these intruders with a large imaginary level shift, the resulting smoothed curve has a very different shape in the stretched region and is not entirely satisfactory. It should not be surprising that the quality of the cud-SC-NEVPT2 curve degrades at longer distances. At such stretched geometries, there are many fractional occupation numbers and consequently, the three-particle and four-particle density matrices are less diagonally dominant, even in the natural orbital basis. Thus, the amount of information provided by incorporating the diagonal elements of these quantities is decreased.

In Table V, we show the spectroscopic constants (obtained by numerical fitting of the potential energy curve) for the $^1\Sigma_g$ and $^3\Sigma_u$ states of N_2. While the bare (i.e., without level-shift) cu-SC-NEVPT2 spectroscopic constants are quite poor, application of the imaginary level shift, which smooths over the equilibrium region of the curve, actually produces quite reasonable spectroscopic constants of an accuracy comparable to standard CASPT2 and SC-NEVPT2. Only the dissociation energy is somewhat large, and this can be attributed to the vertical shift of the dissociated region of the curve due to the level shift as discussed above. cud-SC-NEVPT2 spectroscopic constants with or without level shifts are quite reasonable for both states and are again comparable in accuracy to standard CASPT2 and SC-NEVPT2. This reflects the relatively good behavior of the cud-SC-NEVPT2 approximation in the equilibrium region.

In Fig. 6 we show the Cr_2 binding curve computed using SC-NEVPT2 and the cud-SC-NEVPT2 approximation with a variety of imaginary level shifts. In this challenging system, even the cud-SC-NEVPT2 approximation shows strong false intruder behavior in the equilibrium region. By applying successively larger imaginary level shifts, we can smooth out the divergences, but the general quality of the potential energy curve is not so good. At larger level shifts, we obtain a double well with cud-SC-NEVPT2 rather than the shouldered single-well-type curve that is believed to characterize Cr_2, and, in particular, the well at longer bond distances appears deeper than the well at the normal Cr_2 bond length. It should be noted, however, that the Cr_2 binding curve is very sensitive to the level of theory employed, and, for example, SC-NEVPT3,[43] CIPT2,[44] and internally contracted CI using the *n*-electron valence states[43] all produce curves with a double well structure not unlike our approximate cud-SC-NEVPT2 curve.

TABLE V. Spectroscopic constants for the nitrogen molecule.

N_2 $^1\Sigma_g$			
Method	r_e (Å)	D_e (eV)	ω_e (cm^{-1})
Expt.	1.0977	9.91	2359
CASSCF	1.1069	9.23	2496
CASPT2	1.1012	9.51	2454
SC-NEVPT2	1.1021	9.77	2460
cu-SC-NEVPT2(0.0)	1.1537	11.24	3930
cu-SC-NEVPT2(1.2)	1.0980	9.94	2470
cud-SC-NEVPT2(0.0)	1.1002	9.87	2466
cud-SC-NEVPT2(1.2)	1.0997	9.98	2467
N_2 $^3\Sigma_u$			
Method	r_e (Å)	D_e (eV)	ω_e (cm^{-1})
Expt.	1.2866	3.68	1461
CASSCF	1.3027	2.79	1548
CASPT2	1.2879	3.56	1513
SC-NEVPT2	1.2905	3.54	1522
cud-SC-NEVPT2(0.0)	1.2922	3.78	1521
cud-SC-NEVPT2(0.7)	1.2917	3.79	1522
cud-SC-NEVPT2(1.2)	1.2892	3.82	1524

C. Test case III: Excited states in polyenes

An area of considerable success for multireference perturbation theory calculations, particularly those employing CASPT2 or MRMP theory, has been the description of ex-

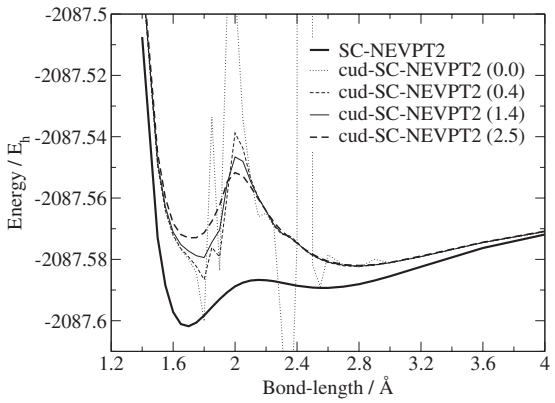

FIG. 6. Cr_2 binding curve using cud-SC-NEVPT2 and SC-NEVPT2 theories. The cud-SC-NEVPT2 calculations are carried out using a variety of imaginary level shifts in the $(-1)'$ subspace (value indicated in brackets).

TABLE VI. Low-lying valence excitations in short-chain polyenes with CASSCF, SC-NEVPT2, cu-SC-NEVPT2, and cud-SC-NEVPT2 methods. Basis and geometry described in text.

		Energy (E_h)	Excitations (eV)			
Molecule	Method	$1A_g^-$	$2A_g^-$	$3A_g^-$	$1B_u^-$	$1B_u^+$
C_4H_6	Expt.					6.25,[a] 5.92[b]
	CASSCF	−154.988 80	6.75	10.93	13.20	8.46
	CASPT2	−155.476 83	6.49	8.14	10.84	6.27
	SC-NEVPT2	−155.486 15	6.91	9.25	11.30	6.46
	cu-SC-NEVPT2	−155.483 33	6.75	8.86	11.19	6.20
	cud-SC-NEVPT2	−155.482 30	6.80	8.66	11.41	6.35
C_6H_8	Expt.					4.93,[c] 4.95,[c] 5.13[d]
	CASSCF	−231.910 53	5.61	8.79	6.77	7.37
	CASPT2	−232.636 34	5.21	8.35	6.32	5.08
	SC-NEVPT2	−232.649 38	5.60	9.00	6.80	5.35
	cu-SC-NEVPT2	−232.644 34	5.38	8.75	6.65	5.12
	cud-SC-NEVPT2	−232.641 34	5.37	8.81	6.60	5.13
C_8H_{10}	Expt.		3.54[e]			4.41[f]
	CASSCF	−308.832 37	4.83	6.73	6.03	6.70
	CASPT2	−309.795 36	4.35	6.05	5.47	4.40
	SC-NEVPT2	−309.813 13	4.71	6.67	5.94	4.47
	cu-SC-NEVPT2	−309.804 88	4.44	6.42	5.68	3.69
	cud-SC-NEVPT2	−309.799 06	4.30	6.30	5.56	4.04
$C_{10}H_{12}$	Expt.		3.48[g]			4.02[g]
	CASSCF	−385.753 57	4.20	6.11	5.27	6.22
	CASPT2	−386.955 68	3.68	5.39	4.70	3.91
	SC-NEVPT2	−386.977 63	4.03	6.01	5.15	3.90
	cu-SC-NEVPT2	−386.966 67	3.59	5.66	4.86	3.52
	cud-SC-NEVPT2	−386.955 49	3.40	5.39	4.42	3.28

[a]Reference 51.
[b]References 52–54.
[c]References 55 and 56.
[d]References 57 and 58.
[e]Reference 59.
[f]References 60 and 61.
[g]Reference 62.

cited states of small to medium sized organic molecules.[45,46] Recently, many examples of successful applications of NEVPT2 to organic molecules have also been reported.[16,47,48] A particularly interesting case that deserves mentioning is the investigation of the absorption spectrum of free base porphin with NEVPT2.[4] As examples of medium sized organic molecules, here we have chosen short-chain polyenes to assess the behavior of the cumulant approximations to SC-NEVPT2.

The geometries of the C_4H_6, C_6H_8, C_8H_{10}, and $C_{10}H_{12}$ in the all-trans configurations were optimized at the density functional theory/B3LYP (Refs. 49 and 50) using Dunning, Jr.'s cc-pVDZ basis.[39,40] The subsequent wave function calculations were carried out in Dunning, Jr.'s cc-pVDZ basis. The CASSCF was chosen to be the full π-valence space. The excited CASSCF states as listed in Table VI for the NEVPT2 calculations were obtained by state-specific CASSCF using the DALTON CASSCF algorithm, while the excited CASSCF states for the CASPT2 comparison calculations were obtained through state-averaged CASSCF using the MOLPRO CASSCF algorithm. For the state-averaged CASSCF, the state average incorporated the lowest three states of A_g symmetry (for the A_g calculations) and the lowest two states of B_u symmetry (for the B_u calculations) while the CASPT2 correction was calculated in a state-specific way (i.e., the density matrix of the given state rather than the average density matrix was used in the construction of the zeroth-order Hamiltonian). The CASPT2 calculations used the rs2c variant as implemented in MOLPRO. In all CASPT2 and NEVPT2 calculations the σ electrons were correlated as core orbitals.

1. Discussion

The primary effect of dynamical correlation on the low-lying valence excited states in polyenes is to lower the energy of the "ionic" excited state $1B_u^+$ relative to the covalent excited states $2A_g^-$, $3A_g^-$, and $1B_u^-$. Of particular interest is the crossing point, i.e., the length of polyene at which the $1B_u^+$ state becomes degenerate with the $2A_g^-$ state. Comparing the cu-SC-NEVPT2, cud-SC-NEVPT2, and parent SC-NEVPT2 methods in Table VI, we observe that the cumulant approximated methods do reproduce the lowering of the $1B_u^+$ state

relative to the covalent excited states (as compared to CASSCF). Furthermore, the cu-SC-NEVPT2 and cud-SC-NEVPT2 preserve the state ordering of the parent SC-NEVPT2 method, and with these methods the $1B_u^+$ and $2A_g^-$ states become nearly degenerate in $C_{10}H_{12}$ just as in the parent SC-NEVPT2 method. The cumulant approximated excitation energies are consistently too low compared to the SC-NEVPT2 excitation energies, and this underestimation appears to get worse as the polyene chain gets longer. Most of the excitation error can be traced to the error in the ground-state energy: both cu-SC-NEVPT2 and cud-SC-NEVPT2 place the energy of the ground state too high, leading to an overall decrease in all the excitation energies. Examining the contributions of the different subspaces, once again we observe that the largest error in the cumulant approximated methods occurs in the $(-1)'$ subspace. Unlike in the previous test cases, the cud-SC-NEVPT2 method does not perform any better than the cu-SC-NEVPT2 method. Overall, we observe that the cumulant approximated theories give a qualitatively reasonable picture of the excitation energies in these conjugated molecules, although the quantitative accuracy for large conjugated systems remains to be seen.

IV. CONCLUSIONS

In the current work, we have explored the possibility of constructing approximations to multireference perturbation theory that do not depend on three- and four-particle density matrices, with the view to enabling dynamical correlation calculations in conjunction with very large active spaces. As our parent multireference perturbation theory, we have investigated the strongly contracted variant of the *n*-electron valence perturbation theory. Our strategy has been to employ cumulant-type approximations to the three- and four-particle density matrices that appear in the formulation using the one- and two-particle density matrices and quantities of similar complexity. We have proposed two cumulant approximated methods: cu-SC-NEVPT2 and cud-SC-NEVPT2. The latter incorporates additional exact information about diagonal and off-diagonal elements of the three- and four-particle density matrices with the same complexity $O(n_{\mathrm{act}}^4)$ as the two-particle density matrices. We find that an undesirable feature introduced by using cumulant approximations is the re-emergence of intruder states in the perturbation theory (which do not usually appear in the SC-NEVPT2 theory) due to the inaccurate representation of denominators by their cumulant approximated form. We have assessed the cumulant approximations in several benchmark test systems. We find that the cumulant approximated methods, when augmented by appropriate level shifts to deal with possible intruder state problems, do provide a qualitatively correct picture of dynamical correlation in many cases. We find also that the cud-SC-NEVPT2 theory has much weaker intruder state problems than the pure cumulant cu-SC-NEVPT2 theory. The accuracy of the cumulant approximated theories is necessarily degraded from the parent multireference perturbation theory, although in many cases the cumulant derived error is within the intrinsic error range associated with multireference second-order perturbation theory. While the cumulant approximated theories may be used with care as a practical means to obtain information on qualitative effects of dynamical correlation in systems with many active orbitals where the parent multireference perturbation theories cannot be applied, we would clearly like more reliable approximations to the denominators in the SC-NEVPT2 method. Work in this direction is underway.

ACKNOWLEDGMENTS

This work was supported by the National Science Foundation CAREER program (Grant No. CHE-0645380) and the Department of Energy, Office of Science (through Award No. DE-FG02-07ER46432).

[1] K. Andersson, P. Å. Malmqvist, and B. O. Roos, J. Chem. Phys. **96**, 1218 (1992).
[2] Y.-K. Choe, Y. Nakao, and K. Hirao, J. Chem. Phys. **115**, 621 (2001).
[3] C. Angeli, R. Cimiriglia, S. Evangelisti, T. Leininger, and J.-P. Malrieu, J. Chem. Phys. **114**, 10252 (2001).
[4] C. Angeli, M. Pastore, and R. Cimiriglia, Theor. Chem. Acc. **117**, 743 (2007).
[5] S. R. White and R. L. Martin, J. Chem. Phys. **110**, 4127 (1999).
[6] K. H. Marti, I. M. Ondik, G. Moritz, and M. Reiher, J. Chem. Phys. **128**, 014104 (2008).
[7] D. Zgid and M. Nooijen, J. Chem. Phys. **128**, 144115 (2008).
[8] D. Zgid and M. Nooijen, J. Chem. Phys. **128**, 144116 (2008).
[9] D. Ghosh, J. Hachmann, T. Yanai, and G. K.-L. Chan, J. Chem. Phys. **128**, 144117 (2008).
[10] J. Hachmann, J. J. Dorando, M. Aviles, and G. K.-L. Chan, J. Chem. Phys. **127**, 134309 (2007).
[11] J. Hachmann, W. Cardoen, and G. K.-L. Chan, J. Chem. Phys. **125**, 144101 (2006).
[12] G. K.-L. Chan, J. Chem. Phys. **120**, 3172 (2004).
[13] P.-Å. Malmqvist, A. Rendell, and B. O. Roos, J. Phys. Chem. **94**, 5477 (1990).
[14] D. Walter and E. A. Carter, Chem. Phys. Lett. **346**, 177 (2001).
[15] P. Celani and H. J. Werner, J. Chem. Phys. **112**, 5546 (2000).
[16] R. W. A. Havenith, P. R. Taylor, C. Angeli, R. Cimiraglia, and K. Ruud, J. Chem. Phys. **120**, 4619 (2004).
[17] W. Kutzelnigg and D. Mukherjee, J. Chem. Phys. **107**, 432 (1997).
[18] F. Colmenero and C. Valdemoro, Phys. Rev. A **47**, 979 (1993).
[19] H. Nakatsuji and K. Yasuda, Phys. Rev. Lett. **76**, 1039 (1996).
[20] D. A. Mazziotti, Phys. Rev. A **57**, 4219 (1998).
[21] *Reduced-Density-Matrix Mechanics with Application to Many-Electron Atoms and Molecules*, Advanced Chemical Physics Vol. 134, edited by D. A. Mazziotti (Wiley, New York, 2007).
[22] T. Yanai and G. K.-L. Chan, J. Chem. Phys. **127**, 104107 (2007).
[23] T. Yanai and G. K.-L. Chan, J. Chem. Phys. **124**, 194106 (2006).
[24] S. R. White, J. Chem. Phys. **117**, 7472 (2002).
[25] C. Angeli, R. Cimiriglia, and J.-P. Malrieu, J. Chem. Phys. **117**, 9138 (2002).
[26] C. Angeli, R. Cimiriglia, and J.-P. Malrieu, Chem. Phys. Lett. **350**, 297 (2001).
[27] K. G. Dyall, J. Chem. Phys. **102**, 4909 (1995).
[28] D. A. Mazziotti, Phys. Rev. A **57**, 4219 (1998).
[29] L. Cohen and C. Frishberg, Phys. Rev. A **13**, 927 (1976).
[30] H. Nakatsuji, Phys. Rev. A **14**, 41 (1976).
[31] F. E. Harris, Int. J. Quantum Chem. **90**, 105 (2002).
[32] J. M. Herbert, Int. J. Quantum Chem. **107**, 703 (2007).
[33] N. Forsberg and P. Å. Malmqvist, Chem. Phys. Lett. **274**, 196 (1997).
[34] DALTON, a molecular electronic structure program, Release 2.0, 2005, see http://www.kjemi.uio.no/software/dalton/dalton.html.
[35] H.-J. Werner, P. J. Knowles *et al.*, MOLPRO, Version 2008.1, a package of *ab initio* programs, 2008, see http://www.molpro.net.
[36] C. W. Bauschlicher, Jr. and P. R. Taylor, J. Chem. Phys. **85**, 6510 (1986).
[37] C. W. Bauschlicher, Jr. and P. R. Taylor, J. Chem. Phys. **86**, 1420 (1987).
[38] B. O. Roos and K. Andersson, Chem. Phys. Lett. **245**, 215 (1995).
[39] T. H. Dunning, Jr., J. Chem. Phys. **90**, 1007 (1989).
[40] K. L. Schuchardt, B. T. Didier, T. Elsethagen, L. Sun, V. Gurumoorthi, J. Chase, J. Li, and T. L. Windus, J. Chem. Inf. Model. **47**, 1045 (2007).

[41] A. J. H. Wachters, J. Chem. Phys. **52**, 1033 (1970).
[42] C. W. Bauschlicher, Jr., S. R. Langhoff, and L. A. Barnes, J. Chem. Phys. **91**, 2399 (1989).
[43] C. Angeli, B. Bories, A. Cavallini, and R. Cimiraglia, J. Chem. Phys. **124**, 054108 (2006).
[44] P. Celani, H. Stoll, H.-J. Werner, and P. Knowles, Mol. Phys. **102**, 2369 (2004).
[45] B. O. Roos, K. Andersson, M. P. Fülscher, L. Serrano-Andrés, K. Pierloot, M. M. Merchán, and V. Molina, J. Mol. Struct.: THEOCHEM **388**, 257 (1996).
[46] K. Nakayama, H. Nakano, and K. Hirao, Int. J. Quantum Chem. **66**, 157 (1998).
[47] M. Pastore, C. Angeli, and R. Cimiriglia, Chem. Phys. Lett. **422**, 522 (2006).
[48] M. Pastore, C. Angeli, and R. Cimiriglia, Chem. Phys. Lett. **426**, 445 (2006).
[49] A. D. Becke, J. Chem. Phys. **98**, 5648 (1993).
[50] C. Lee, W. Yang, and R. Parr, Phys. Rev. B **37**, 785 (1988).
[51] R. McDiarmid, Chem. Phys. Lett. **188**, 423 (1992).
[52] J. P. Doering and R. McDiarmid, J. Chem. Phys. **73**, 3617 (1980).
[53] J. P. Doering and R. McDiarmid, J. Chem. Phys. **75**, 2477 (1981).
[54] O. A. Mosher, W. M. Flicker, and A. Kuppermann, Chem. Phys. Lett. **19**, 332 (1973).
[55] R. M. Gavin, S. Risemberg, and S. A. Rice, J. Chem. Phys. **58**, 3160 (1973).
[56] R. M. Gavin and S. A. Rice, J. Chem. Phys. **60**, 3231 (1974).
[57] A. Kuppermann, W. M. Flicker, and O. A. Mosher, Chem. Rev. (Washington, D.C.) **79**, 77 (1979).
[58] W. M. Flicker, O. A. Mosher, and A. Kuppermann, Chem. Phys. Lett. **45**, 492 (1977).
[59] M. Granville, G. Holtom, B. Kohler, R. Christensen, and K. D'Amico, J. Chem. Phys. **70**, 593 (1979).
[60] L. A. Heimbrook, B. E. Kohler, and I. J. Levy, J. Chem. Phys. **81**, 1592 (1984).
[61] D. G. Leopold, R. D. Pendley, J. L. Roebber, R. J. Hemley, and V. J. Vaida, J. Chem. Phys. **81**, 4218 (1984).
[62] L. D'Amico, C. Manos, and R. L. Christensen, J. Am. Chem. Soc. **102**, 1777 (1980).